Modifications to Risk-Targeted Seismic Design Maps for Subduction and Near-Fault Hazards

Abbie B. Liel
Assistant Prof., Dept. of Civil, Environ. and Arch. Eng., University of Colorado, Boulder, CO, USA

Nicolas Luco
Research Structural Engineer, U.S. Geological Survey, Golden, CO, USA

Meera Raghunandan
Structural Engineer, RSE Associates Inc., Watertown, MA, USA

Casey P. Champion
Structural Engineer, ZFA Structural Engineers, San Francisco, CA, USA

ABSTRACT: ASCE 7-10 introduced new seismic design maps that define risk-targeted ground motions such that buildings designed according to these maps will have 1% chance of collapse in 50 years. These maps were developed by iterative risk calculation, wherein a generic building collapse fragility curve is convolved with the U.S. Geological Survey hazard curve until target risk criteria are met. Recent research shows that this current approach may be unconservative at locations where the tectonic environment is much different than that used to develop the generic fragility curve. This study illustrates how risk-targeted ground motions at selected sites would change if generic building fragility curve and hazard assessment were modified to account for seismic risk from subduction earthquakes and near-fault pulses. The paper also explores the difficulties in implementing these changes.

1. INTRODUCTION

Seismic design maps adopted by building codes in the U.S. have recently moved from a philosophy of uniform hazard to a philosophy of uniform risk. ASCE 7 2005 maps ground shaking intensities that have 2% probability of exceedance in 50 years at sites throughout the country (ASCE 2005a). Despite being designed for uniform hazard, differences in the shape of seismic hazard curves at different sites and uncertainties in building collapse capacities produce non-uniform risk of collapse for buildings across the country. Based on this observation and the uniform risk philosophy in the ASCE 43-05 Standard for nuclear facilities (ASCE 2005b), Luco *et al.* (2007) proposed a risk-targeted approach for determining seismic design values, which has been adopted by ASCE 7 2010 (ASCE 2010). For code-designed buildings, the maps target a 1% probability of collapse in 50 years.

The collapse probability is determined by convolving a building collapse fragility, $P[Col/Sa =a]$, with the seismic hazard curve, $\lambda[Sa>a]$, at a particular site:

$$\lambda[Col] = \int_0^\infty \frac{dP[Col|Sa=a]}{da} \lambda[Sa > a]da \quad (1)$$

where $\lambda[Col]$ is the mean annual frequency of collapse and *Sa* is the pseudo spectral acceleration. $\lambda[Col]$ is coupled with a Poisson assumption for collapse occurrence to arrive at the collapse probability in 50 years.

In developing the risk-targeted ground motion maps, a generic collapse fragility is defined for code-designed buildings. The generic fragility assumes buildings have 10% probability of collapse under the mapped ground motion values for which they were designed. This 10% probability of collapse was estimated by the

FEMA P695 project for modern code-conforming buildings (FEMA 2009). The uncertainty in the collapse fragility curve, assuming a lognormal distribution, is quantified by a lognormal standard deviation of 0.6.

The risk-targeted seismic design maps were developed iteratively. First, the collapse fragility was determined with the existing Maximum Considered Earthquake (*MCE*) spectral values, and convolved with the hazard curve. If the probability of collapse produced differed from the target 1% in 50 years, the *MCE* ground motion intensity was modified and the calculation repeated. These calculations were carried out considering structures with fundamental periods of vibration of 0.2 s and 1 s. The outcome of this process was a set of risk-targeted *MCE* ground motion intensities, denoted MCE_R, which provide the basis for the mapped values in the 2010 version of ASCE 7 (ASCE 2010). The introduction of the risk-targeted values led to a reduction in design ground motions by around 15% in some areas, and minor changes in other parts of the country.

The adoption of the risk-targeted maps by ASCE 7 and the International Building Code (IBC) marked a significant change in design philosophy toward the idea of uniform risk. However, it is important to recognize that the methods used to determine the risk-targeted values are based on a number of assumptions. One assumption involves the application of the same generic collapse fragility curve for code-designed buildings at all locations in the U.S. Recent work by Raghunandan *et al.* (2014) suggests that this fragility curve may not be appropriate at locations that are affected by subduction zone earthquakes, because buildings appear to be more fragile when subjected to the long duration shaking that is a characteristic of subduction events (see also Chandramohan *et al.* 2015). The risk-targeted approach also does not capture the near-fault conditions associated with directivity effects that may produce pulse-like ground motions. Such motions impact both the fragility and hazard curves that go into the risk

determination (Champion and Liel 2012). This paper further advances the risk-targeted seismic design maps by exploring how recent research could be used to enhance the treatment of (a) subduction and (b) near-fault hazard conditions in these maps.

2. COLLAPSE RISK AT SITES AFFECTED BY SUBDUCTION EARTHQUAKES

The Pacific Northwest U.S. (including Oregon, Washington and Alaska) has experienced both subduction and crustal earthquakes. Ground motions from subduction earthquakes are generally longer in duration as compared to ground motions from the more frequently recorded and studied shallow crustal events. The long duration comes from the higher magnitudes expected from subduction events and the deep epicenter, which produces greater source-to-site distances as compared to crustal earthquakes (Bommer *et al.* 2009). The generic fragility curve used in developing the risk-targeted seismic design maps was generated using ground motions from crustal earthquakes.

2.1. Collapse Risk Assessment Considering Subduction Earthquakes

Failing to consider the unique features of subduction ground shaking can lead to underestimation of collapse risk at locations where subduction sources contribute sub-stantially to the hazard. To examine this effect, Raghunandan *et al.* (2014) designed 2-, 4- and 8-story reinforced concrete special moment resisting frame buildings according to the 2012 IBC for sites in Seattle, WA (47.6°N, 122.3°W) and Portland, OR (45.5°N, 122.65°W). Non-linear models of each building were developed and subjected to two suites of recorded ground motions using incremental dynamic analysis: (1) a set of recordings from crustal earthquakes, and (2) a set of recordings from subduction earthquakes. (Note that, in both cases, the recordings are scaled in incremental dynamic analysis. The likelihood of actually observing such scaled intensities is taken into account on the hazard side of the calculation.)

Collapse capacity is quantified by the spectral acceleration at the fundamental period of the building needed to cause collapse. Table 1 reports the median collapse capacities (spectral acceleration causing 50% probability of collapse) obtained in each case. The collapse assessments show that all of the buildings are more fragile when subjected to subduction records, as compared to the crustal records, exhibiting an apparent average 38% reduction in collapse capacity. The record-to-record variability in collapse capacity is on the order of 0.38 for the crustal ground motion set, and on the order of 0.42 for the subduction set. The increase in variability associated with the subduction set likely stems from the wide range of ground motion durations among the subduction records.

Table 1: Collapse Capacities, in terms of Sa(T₁)

Bldg., Num. of Stories /City	First-Mode Period*, T_1 [sec]	Median Collapse Capacity, Sa(T_1) [g]	
		Crust.	Subd.
2/Seattle	0.58	4.4	2.2
4/Seattle	1.0	2.4	1.5
8/Seattle	1.8	1.2	0.84
2/Portland	0.63	3.6	2.1
4/Portland	1.0	2.4	1.5
8/Portland	2.0	1.1	0.79

* Obtained from eigenvalue analysis of nonlinear models with cracked section properties

The collapse risk of these buildings was determined by applying the risk integral in Equation 1 twice, such that the seismic hazard from subduction sources at the site was convolved with the subduction collapse fragility, and the seismic hazard from crustal sources at the site was convolved with the corresponding fragility curve. Then the annual frequencies of collapse from both events were added (Raghunandan *et al.* 2014). This calculation requires the hazard at each site to be deaggregated by subduction and crustal sources and the separate collapse fragility curves for the two ground motion suites.

In this paper, the computation is made considering the hazard and fragility both defined at $T = 1$ s. The subduction and crustal fragility curves are both assumed to have a total uncertainty (logarithmic standard deviation) of 0.60, accounting for record-to-record and modeling variability.

The 50-year collapse probabilities obtained through this approach are shown in Table 2. Table 2 also lists the probability of collapse in 50 years when the crustal collapse fragility is used to calculate both the crustal and subduction results. These values show that the collapse risk may be underestimated by 40-65% if the higher fragility of buildings under long duration subduction shaking is not considered.

These collapse probabilities cannot be directly compared to the 1% probability of collapse in 50 year target for a number of reasons (e.g., assumptions made in the design process that may have contributed to conservative designs, buildings designed and analyzed for site class D, collapse fragilities computed with an adjustment for spectral shape). However, in the next section we show how the relative difference between the crustal and subduction collapse fragility curves from this study can be used to inform updated risk-targeted maps.

Table 2: Probability of Collapse in 50 years

Bldg., Num. of Stories/Site	P[Col] in 50 years [%]	P[Col] in 50 years w/o considering Subd. Fragility [%]
2/Seattle	0.62	0.22
4/Seattle	0.51	0.19
8/Seattle	0.30	0.17
2/Portland	0.47	0.22
4/Portland	0.41	0.14
8/Portland	0.21	0.11

2.2. Accounting for these Effects in Risk-Targeted Seismic Design Maps

We propose the following process for risk-targeted mapping at sites where subduction and crustal sources contribute to seismic hazard:

- Before computing the risk integral, the

hazard is deaggregated by subduction and crustal sources. This information is simply a deaggregation of existing U.S. Geological Survey (USGS) hazard calculations, and accounts for the relative significance of the crustal and subduction sources at a site.

- The generic fragility curve for crustal events is assumed to have 10% probability of collapse under MCE_R ground shaking, following Luco *et al.* (2007). The logarithmic standard deviation of the fragility is taken as 0.60, which is from the same reference.

- The generic fragility used for subduction events is assumed to have a median collapse capacity that is a fraction k of the median capacity considering crustal events (*i.e.*, $m_s = k \cdot m_c$). Comparing the values in the third and fourth column of Table 2 for m_s and m_c suggests that $k = 0.65$ may be appropriate.

- The value of MCE_R is subsequently varied until the probability of collapse in 50 years is approximately 1%, producing the risk-targeted ground motion at each site.

This approach is used to compute risk-targeted ground motions for the Portland and Seattle sites, with the results listed in Table 3. These calculations are carried out for the spectral acceleration at $T = 1$s and for soil site class D.[1] The first column of values in Table 3 reports the risk-targeted ground motions that we would obtain if the differences between subduction and crustal fragilities are not considered in the analysis, *i.e.*, consistent with the current map approaches. If the median collapse capacity of the subduction generic fragility (m_s) is assumed to be 35% less than median collapse capacity of the crustal generic fragility (m_c), *i.e.*, $k = 0.65$, the MCE_R values to be used for design increase by about 0.2g. Table 3 also shows how the MCE_R values would change if the assumed reduction in median collapse capacity for the subduction fragility is bigger or smaller.

---

[1] In this and the next example, the changes in risk-targeted ground motions are illustrated for site class D. However, mapped values of S_1 are for site class BC, so these numbers are not directly comparable to the current maps.

Table 3: MCE_R at 1 s, in units of g, at example sites affected by subduction sources

Site	MCE_R w/o considering differences in fragility	MCE_R $m_s = 0.5m_c$	MCE_R $m_s = 0.65m_c$	MCE_R $m_s = 0.8m_c$
Seattle	0.62g	1.04g	0.83g	0.71g
Portland	0.52g	0.94g	0.74g	0.62g

2.3. Outstanding Issues

The approach taken in the previous section to adjust risk-targeted ground motions for subduction sources considers two generic fragilities, one to be convolved with the crustal hazard, and a second to be convolved with the subduction hazard. The second generic fragility is defined using a smaller median collapse capacity, consistent with the observed structural response to subduction ground motions.

Of course, the observed shift in collapse capacity between crustal and subduction records depends on characteristics of the buildings and the tectonic environment. First, the $k = 0.65$ value is only appropriate for ductile buildings, such as the special reinforced concrete moment resisting frames used in the example. Raghunandan *et al.* (2014) observed that less ductile buildings show a smaller difference between the crustal and subduction collapse fragilities. The focus on ductile buildings is considered appropriate here because the building systems permitted in high seismic areas of the U.S. are expected to behave in a ductile manner (ASCE 2010).

Second, the difference in collapse fragility between subduction and crustal records is highly sensitive to the duration of subduction motions. In Raghunandan *et al.* (2014), the average duration of the subduction records used in the analysis is 44.3s, compared to 13.9s for the crustal set. Ideally, the risk-targeted ground motion computation would compute the shift in the generic fragilities on the basis of the expected duration of ground shaking at a particular site. Although ground motion prediction equations for duration have been developed (*e.g.* Kempton and Stewart, 2006; Bommer *et al.* 2009), these

relationships would need to be validated for the subduction earthquakes for this purpose.

Third, the subduction hazard as described here combines the hazard from two types of subduction earthquakes: interface (generally $M_w > 8$) and deep intraslab (generally $M_w < 8$) earthquakes (Atkinson and Boore 2003). The intraslab earthquakes are generally of smaller magnitude and may not produce as long duration shaking. As a result, lumping the two subduction sources together may be overly pessimistic. More research is needed to study the effect of these different source contributions.

3. COLLAPSE RISK AT NEAR-FAULT SITES

At sites that are close to active faults, ground motions sometimes exhibit a large pulse near the beginning of the velocity time history. These pulses occur when the fault rupture propagates toward the site, leading to constructive interference of the wave front and the arrival of the seismic energy from the rupture in a large amplitude pulse. Forward directivity decreases with distance from the fault, such that ground motions with these features are unlikely to occur more than 10 to 15 km away from the rupture.

Current seismic design maps do not fully consider the impacts of forward directivity in the hazard and fragility calculations needed to compute risk-targeted ground motions near active faults and, as a result, may underestimate collapse risk at some sites (Champion and Liel 2012). We also note that the risk-targeted ground motions do not always govern at near-fault sites. Instead, the current seismic design maps use a deterministic ground motion intensity from characteristic earthquakes if it is lower than the risk-targeted ground motion. We do not consider this issue directly here, instead focusing on what would be needed to extend the idea of risk-targeted ground motions to sites near active faults, considering the additional complexity associated with quantifying hazard and fragility.

3.1.Collapse Risk Assessment at Near-Fault Sites
The unique pulse characteristics of ground motions near faults greatly complicate both seismic hazard and collapse risk assessments. On the seismic hazard side, models need to consider the likelihood of pulse occurrence and the duration of the pulse ("pulse period"), which depends on site-to-source geometry, earthquake magnitude and other characteristics. Shahi and Baker (2011) proposed a framework for incorporating these directivity effects in probabilistic seismic hazard analysis to predict the probability of a pulse-like ground motion occurring at a site, the expected orientations of the pulse (*i.e.*, directionality), and the response spectrum amplification associated with the pulse.

On the risk assessment side, structural response and collapse depends on the ground motion pulse period and the building's first-mode period. Champion and Liel (2012) conducted nonlinear collapse analysis of 23 reinforced concrete special moment frame buildings using a set of pulse-like ground motions. As Figure 1 shows, the ability of the structure to withstand ground shaking depends highly on the ratio of the pulse period (T_p), to the fundamental period (T_1). The building has lower capacity to resist collapse when the pulse period is longer than the first mode period, which is attributed to lengthening of the building period (from nonlinear deformations) into a range that coincides with the pulse period.

Champion and Liel (2012) show that, for near-fault conditions, the collapse fragility depends on the probability of a pulse occurring and the corresponding pulse period, and the probability of collapse conditioned on each pulse period of interest. This component of the fragility is combined with collapse probabilities associated with far-field (non-pulse) ground motions to arrive at a total probability of collapse. Through this approach, the near-fault collapse fragility curves depend on both site characteristics (pulse-period distribution) and building characteristics.

Table 4 reports the median collapse capacities obtained by Champion and Liel (2012) for 2- to 20-story modern special reinforced

concrete space frames, computed for a site 5 km from the Imperial Valley fault (32.78°N, 115.40°W). The results show that buildings tend to be more fragile when the collapse fragility is computed considering the possibility of pulses occurring. However, the significance of the near-fault effect depends on the building's first-mode period. On average, the median collapse capacities are 15% lower when pulse-like motions are considered in the development of the collapse fragilities. We note the record-to-record variability from the near-fault collapse analyses is on average 0.46, while those computed for the conventional far-field fragilities average to 0.40.
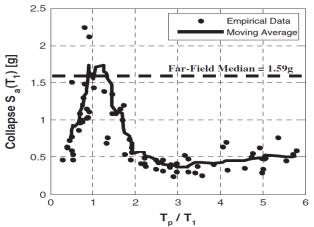

Figure 1: Response of an 8-story special moment resisting frame building subjected to 91 earthquake records with pulses, showing collapse capacity as a function of the ratio of ground motion pulse period to building period (from Champion and Liel 2012).

Table 4: Collapse Capacities, in terms of Sa(T₁)

Bldg. (Num. of Stories)	First-Mode Period*, T_1 [sec]	Median Collapse Capacity, $Sa(T_1)$ [g]	
		Near-Fault	Far-Field
2	0.60	4.60	4.87
4	0.91	3.24	3.01
8	1.81	1.12	1.59
12	2.15	0.84	1.12
20	2.53	0.91	1.03

The collapse risk of these buildings is determined by combining the near-fault fragility curves with a seismic hazard curve that

incorporates directivity and pulse occurrence. For the purpose of illustration in this paper, the fragility curves are assumed to have an uncertainty (logarithmic standard deviation) of 0.60, combining record-to-record variability and modeling uncertainty. The 50-year collapse probabilities obtained through this approach considering near-fault (NF) hazard and NF fragility curves are illustrated in Figure 2 (labeled "Case D"). Figure 2 also depicts the impact of excluding near-fault directivity from the hazard and fragility curves for three other cases. (Cases A, B and C are as described in Section 3.2 except that the collapse fragility curves are from Champion and Liel (2012) rather than the generic fragilities used for the risk-targeted mapping).
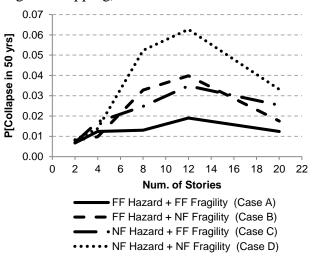

Figure 2: Probability of collapse in 50 years for buildings at the Imperial Valley site, considering different assumptions in the development of collapse fragility and hazard curves (Cases A-D; see text).

Figure 2 shows that the inclusion of near-fault effects is not significant for the shorter structures ($T_1 < ~1$ s). However, for the taller buildings, the possible occurrence of pulse-like ground motions greatly alters the collapse risk assessment, and the fully inclusive near-fault assessment (Case D) indicates risks of 3-6% probability of collapse in 50 years. Comparing Cases B and C, we observe that inclusion of near-fault fragility and near-fault hazard seem to

be equally important for the quantification of collapse risk.

We note that these results are not directly comparable to the target of 1% probability of collapse in 50 years used for the current seismic design maps because the buildings were designed for smaller seismic forces than indicated by the mapped values at that site, and the design and analysis were conducted for site class D. Nonetheless, a relative comparison of the results for Cases A and D shows collapse risks for taller structures can increase by a factor of 2 to 4 when near-fault effects are incorporated into the assessment.

3.2. Accounting for these Effects in Risk – Targeted Seismic Design Maps

We explore the impacts of near-fault collapse fragility and hazard on risk-targeted ground motions for the Imperial Valley site using four different sets of assumptions, with the results shown in Table 5.

- Case A: Convolves a hazard curve from Shahi and Baker (2011) that does not consider near-fault effects, and the generic fragility curve assumed to have 10% probability of collapse under MCE_R ground shaking and a lognormal standard deviation of 0.6. The hazard calculated by Shahi and Baker (2011) is similar to the USGS hazard used in current design maps, such that Case A is essentially consistent with the current seismic design maps where the deterministic cap does not govern.
- Case B: Convolves a hazard curve from Shahi and Baker (2011) that does not consider near-fault effects, and a generic fragility curve that is defined based on typical near-fault response obtained by Champion and Liel (2012). This typical near-fault fragility curve is based on results at the Imperial Valley site, and considers a 15% reduction in the median collapse capacity from the generic fragility in Case A and a lognormal standard deviation of 0.6.
- Case C: Convolves a near-fault hazard curve from Shahi and Baker (2011), and the generic

fragility curve assumed to have 10% probability of collapse under MCE_R shaking.
- Case D: Convolves a near-fault hazard curve from Shahi and Baker (2011), and the generic near-fault fragility curve defined in Case B. Case D represents complete treatment of near-fault effects.

Table 5: MCE_R at 1 sec, in units of g, the Imperial Valley near-fault site with different assumptions

MCE_R Case			
A	B	C	D
1.30g	1.54g	1.46g	1.72g

The risk-targeted calculations are carried out for a spectral acceleration at 1 s and for site class D. The first column in Table 5 reports the risk-targeted ground motion that we would obtain if the unique characteristics of near-fault sites are not considered in the analysis, *i.e.*, consistent with the current map approaches. Consideration of directivity and pulse-like ground motions in both the hazard and fragility (Case D) increases the design ground motion by about 0.4 g for this site, which is a substantial change. However, since the pulse-like ground motions that can occur near faults have been primarily observed to affect longer period buildings, the calculated increase would only apply to risk-targeted spectral accelerations at 1 s and not at 0.2 s.

3.3. Outstanding Issues

The results in Table 5 show the impact of different sets of assumptions in the computation of risk-targeted ground motions near active faults. However, we note that, at the present time, there are barriers to all of these approaches with the exception of Case A.

Cases B and D use readily available hazard information, but require a near-fault fragility curve. This near-fault fragility curve is complicated because it depends on both site and building characteristics. The relevant site features are the distributions of pulse periods associated with different ground motion intensity levels, which is provided by near-fault probabilistic seismic hazard analysis. The

relevant building features are the building's deformation capacity and the first-mode period. We assume that all modern code-designed buildings have similarly large deformation capacities. However, there will be significant variation in building periods. Data from Champion and Liel (2012) and Table 4 suggest that near-fault effects are more significant for longer period buildings, but this conclusion may also depend on the pulse period distribution that different faults are likely to generate (and resulting T_P / T_1 values). The development of a generic near-fault fragility curve would require exploration of the site and building effects at a greater number of sites to explore the impact of these characteristics for collapse assessment and risk-targeted mapping.

Cases C and D use probabilistic seismic hazard analyses that incorporate directivity and pulses that can occur near active faults, unlike the USGS National Seismic Hazard Model. The NGA West 2 project on ground motion prediction equations included a working group on directivity, but concluded more extensive comparison of models is still needed (Bozorgnia *et al.* 2014).

4. CONCLUSIONS

This paper shows how new knowledge about the impacts of (a) long duration shaking from subduction earthquakes and (b) pulse-like ground motions occurring very close to faults on the collapse risk of buildings can be incorporated in the risk-targeted seismic design maps. For subduction earthquakes, deaggregation of the hazard by subduction and crustal sources, and a modified generic fragility is needed that accounts for the higher collapse risk of buildings if the duration of shaking is very long. At the example sites, this appears to increase the design values at 1 s by about 0.2 g. For near-fault sites, modifications to both the generic fragility and the hazard used in the risk-targeted maps are needed. If included, these changes could increase the design values at some sites substantially. More research is needed to determine an appropriate generic fragility curve and to update

hazard calculations in the near-field context.

6. REFERENCES

ASCE (2005a; 2010). Minimum Design Loads for Buildings and Other Structures (ASCE Standard 7-05; 7-10). ASCE, Reston, VA.

ASCE (2005b) Seismic Design Criteria for Structures, Systems and Components in Nuclear Facilities, (ASCE Standard 43-05). ASCE, Reston, VA.

Bommer JJ, *et al.* (2009). Empirical equations for the prediction of the significant, bracketed, and uniform duration of earthquake ground motion. *Bull Seismol Soc Am.*; 99(6):3217–3233.

Bozorgnia, Y et al. (2014). NGA-West2 Research Project. *Earthquake Spectra* 30(3), 973-987.

Champion, CP, Liel, AB. (2012). The effect of near-fault directivity on seismic collapse risk, *Earthquake Engineering and Structural Dynamics*, 41(10): 1391-1409.

Chandramohan, R, *et al.* (2015). Quantifying the influence of ground motion duration on structural collapse capacity using spectrally equivalent records *Earthquake Spectra,* In Press.

FEMA. (2009). Quantification of Building Seismic Performance Factors FEMA P695. FEMA.

Kempton JJ, Stewart JP (2006). Prediction equations for significant duration of earthquake ground motions considering site and near-source effects. *Earthquake Spectra* 22(4):985–1013.

Luco N, *et al.* (2007). Risk-targeted versus current seismic design maps for the conterminous United States. *SEAOC 2007 Convention Proceedings.*

Raghunandan, M, Liel, AB and Luco, N (2014). Collapse risk of buildings in the Pacific Northwest due to subduction earthquakes, *Earthquake Spectra,* In Press (http://dx.doi.org/10.1193/012114EQS011M).

Shahi SK, Baker JW. (2011). An empirically calibrated framework for including the effects of near fault directivity in probabilistic seismic hazard analysis. *Bull Seismol Soc Am* ; 101(2):742–755.